Medical Research Archives

ESMED
European Society of Medicine

OPEN ACCESS

Published: June 30, 2023

Citation: Sreedhar A, Zhang C, et al., 2023. Testing the Double Cause Hypothesis for Autoimmune Diseases, Dipalmitoylphosphatidylcholine Should Be Measured in Plasma or Blood Vessels of Diabetes Type, Medical Research Archives, [online] 11(6). https://doi.org/10.18103/mra.v11i6.3938

DOI
https://doi.org/10.18103/mra.v11i6.3938

ISSN: 2375-1924

RESEARCH ARTICLE

UCP2 Upregulation Increases Fra-1 Expression and S-phase Cell Population without Decreasing Apoptosis during Skin Cell Transformation

Annapoorna Sreedhar[1#], Chunjing Zhang[1,2#], Noel Jacquet[1], Yunfeng Zhao[1,*]

[1] Department of Pharmacology, Toxicology & Neuroscience, LSU Health Sciences Center in Shreveport, Shreveport, LA 71130, USA
[2] School of Basic Medicine, Qiqihar Medical University, Qiqihar, Heilongjiang 161006, China

*Corresponding author
Yunfeng Zhao, Ph.D.
Department of Pharmacology, Toxicology & Neuroscience
LSU Health Sciences Center
1501 Kings Highway
Shreveport, LA 71130-3932
Email: yunfeng.zhao@lsuhs.edu

#Both authors contributed equally to this manuscript

ABSTRACT

Upregulation of uncoupling protein 2 (UCP2) is considered a prosurvival mechanism for cancer cells. This prosurvival function is thought to be mediated by UCP2's uncoupling activity which reduces the production of superoxide in the mitochondria. However, exactly how highly expressed UCP2 regulates cell proliferation, cell cycle, and cell death during the early stage of tumorigenesis has not been studied thoroughly. For this purpose, we generated UCP2 stably overexpressed JB6 Cl-41 cells (a skin cell transformation model) and performed studies to answer the above questions. Our results demonstrated that UCP2 overexpression enhanced cell proliferation, activation of the oncoprotein Fra-1, anchorage-independent growth, 3D spheroids growth, and glucose uptake during skin cell transformation. Next, our results demonstrated that UCP2 overexpression resulted in marked decreases in the proportion of the cells in the G1 phase and an increase of cells in the S phase of the cell cycle, which was accompanied by increased expression of Cyclin E and Cdk2. Lastly, UCP2 overexpression did not enhance or suppress apoptosis during skin cell transformation, as indicated by Annexin V and active caspase 3/7 staining. Taken together, these data suggest that UCP2 upregulation mainly enhances the Fra-1 oncogenic pathway which drives cell proliferation, without inhibiting apoptosis during skin cell transformation.

Keywords: UCP2, skin cell transformation, cell proliferation, apoptosis

Abbreviations used:
UCP2: uncoupling protein 2;
TPA: 12-O-tetradecanoylphorbol-13-acetate
ETC: electron transport chain;
ROS: reactive oxygen species;
FBS: fetal bovine serum
DMSO: dimethyl sulfoxide
PI: propidium iodide
FACS: fluorescence-activated cell sorting
JC-1: 5,5′,6,6′-tetrachloro-1,1′,3,3′-tetraethylbenzimidazol-carbocyanine iodide
AP-1: activator protein 1
PFKFB2: phosphofructokinase 2/fructose -2,6-bisphosphatase 2
PLCγ-1: phospholipase C γ-1

Introduction

Uncoupling proteins (UCPs) are a family of membrane anion transporters localized in the mitochondrial inner membrane. The physiological functions of UCPs include lowering the mitochondrial membrane potential and dissipating the metabolic energy as heat. UCPs disengage the electron transport chain (ETC) from ATP synthesis by decreasing the mitochondrial membrane potential and, as a result, leading to the reduction of superoxide radicals, a byproduct of ETC.[1] Because of this critical role, UCPs are essential for cell survival and proliferation. Among the UCP family members, UCP2 is the only uncoupling protein that is ubiquitously expressed in various tissues including the heart, lung, kidney, liver, spleen, macrophages, and skin.[2] Recent studies suggest that the role of UCP2 may not be limited to uncoupling activity and ROS (reactive oxygen species) regulation. It is also involved in glucose oxidation, fatty acid metabolism, fatty acid export, body weight regulation, and insulin secretion.[3] Because UCP2 plays a pivotal role in these essential cellular processes, dysregulation of UCP2 could contribute to the pathogenesis of certain human diseases such as diabetes, obesity, and cancer.[4,5,6]

In tumor cells, UCP2 and ROS seem to have a complex and sometimes paradoxical association. Elevated levels of ROS are a characteristic feature of almost all tumor cells.[7] However, many types of tumors also amplify the expression levels of UCP2.[8] One explanation is that UCP2 can be activated by increased levels of superoxide; and in turn, elevated levels of UCP2 decrease mitochondrial ROS production, thus contributing to tumor growth and chemoresistance.[6,9] Therefore, the antioxidant effect of UCP2 is of specific importance in cancer progression. Nevertheless, exactly how UCP2 promotes the early stage of tumorigenesis is largely unknown. For this purpose, we have generated UCP2 overexpressed skin epidermal JB6 Cl-41 cells since this cell line is the only well-characterized skin cell model to study tumor promotion.[10]

Alterations in cellular processes may lead to tumorigenesis.[11,12] Defective or dysfunctional mitochondria are one of the major contributors to cancer.[12] Mitochondria stand at the center stage in controlling cellular processes such as ATP synthesis, ROS production, programmed cell death, and in maintaining calcium homeostasis.[13] Therefore, dysfunctional mitochondria cause numerous abnormalities in tumor cell proliferation, cell survival, cell cycle, cell death, and metabolism.[14,15,16] Moreover, cell proliferation, cell survival, and cell death are conserved mechanisms of cell replication leading to cell gain or cell loss respectively. These cellular processes coordinate together to maintain homeostasis.[17] Not surprisingly, an imbalance between these cellular processes can lead to the genesis and progression of cancers.[18,19] UCP2 upregulation, a mitochondrial alteration, has been proposed to be an important contributor to carcinogenesis [4-6]. In our recent studies, using the JB6 Cl-41 skin cell transformation model, we have demonstrated that UCP2 expression is an important regulator of mitochondrial redox balance and cellular bioenergetics.[20,21,22] Furthermore, since ROS play important roles in the regulation of cell proliferation, cell death, and tumorigenesis, we hypothesized that highly expressed UCP2 may promote cell proliferation whereas suppressing apoptosis during skin cell transformation.

Methods

Cell lines, reagents, and treatments

Murine skin epidermal JB6 Cl-41 cells (purchased from American Type Culture Collection) are the only well-characterized skin cell model to study tumor promotion .[10] Cells were grown in an EMEM medium containing 4% fetal bovine serum (FBS), 2 mM L-glutamine, 2.5 μg/ml penicillin, and streptomycin in a 37°C incubator under 5% CO_2. Human UCP2-containing and empty pCMV6 vectors were purchased from OriGene (catalog numbers SC320879 and PS100001, respectively). Vectors were transfected into JB6 cells using the FuGENE transfection reagent (Promega), and stable clones were generated by G418 (200 μg/ml, Sigma) selection. The tumor promoter 12-

O-tetradecanoylphorbol-13-acetate (TPA, Sigma) stock solution (1.6 mM) was prepared in dimethyl sulfoxide (DMSO, Sigma). The final concentration of TPA for cell culture studies was 5 nM. The UCP2 inhibitor genipin was purchased from Cayman Chemical.

Western blot analysis

Collected skin cells were suspended in 250 µl of RIPA buffer containing a proteinase inhibitor cocktail (Santa Cruz Biotechnology). Cells were sonicated on ice for two strokes (10 sec per stroke) using a Fisher Sonic Dismembrator (Model 100, Scale 4). After incubating on ice for 30 min, cell lysate was centrifuged at 18,000 x g for 20 min, and the supernatant was collected and designated as Whole Cell Lysate. The prepared whole cell lysates were used for Western blot analysis. Whole Cell Lysates were loaded onto an SDS-PAGE gel and transferred onto a nitrocellulose membrane after separation. The membrane was blocked with 5% non-fat milk (Bio-Rad), then probed with 1:1000 diluted antibodies against Fra-1 (SC-605), cyclin E (SC-481), GAPDH (SC-32233), PTEN (sc-7974), or β-actin (SC-47778/) (purchased from Santa Cruz Biotechnology), and UCP2 (#8932), cdk2 (#2546), and p-cdk2 (#2561) (purchased from Cell Signaling), followed by incubation with a 1:2500 diluted HRP-conjugated secondary antibody purchased from Jackson ImmunoResearch. Images were visualized using a ChemiDoc imaging system (Bio-Rad).

Anchorage-independent growth assay in soft agar

A soft agar-based cell transformation assay was carried out in six-well plates. The bottom consisted of 2.5 ml of 0.5% agar for each well. A total of 3×10^4 cells, suspended in 0.75 ml of 0.33% agar in EMEM medium, were layered on top and incubated at 37°C for 10 days. Both layers were supplemented with either TPA (5 nM) or DMSO (vehicle control). The colonies were counted manually after Neutral Red staining. The transformation response was expressed as the number of colonies formed per well.

3D spheroid formation assay

3D spheroids were monitored in real-time by live-cell imaging using the IncuCyte Zoom system (Essen Bioscience Ann Arbor, MI, USA). Briefly, JB6 Cl-41 cells were harvested by trypsinization, counted, and 5,000 cells per well were seeded in a 96-well round bottom clear cell repellent plate (Greiner Bio-One) in a normal culture medium supplemented with 1%Matrigel. Culture plates were centrifuged at 300 ×gfor 5 min and incubated within the IncuCyte incubation chamber at 37°C. Following 24 h of incubation, the treatments were added and images were taken automatically every 4 h at 10x magnification. Spheroids formed over 3 days were analyzed using the IncuCyte Zoom software.

Cell Cycle Analysis

Flow cytometry analysis was performed using 3D spheroid cultures of JB6 Cl-41 cells. The spheroids were starved in serum-free media for 24 h followed by treatment for 24 h with TPA (5 nM) or DMSO (control vehicle). The next day the spheroids were harvested using cell dissociation solution (ThermoFisher Scientific, Cat No. 13151014), and then dissociated into single cells using trypsin-EDTA (0.2%) with gentle manual pipetting. Cells were then fixed in 70% ethanol, stained with propidium iodide (PI), and subjected to fluorescence-activated cell sorting (FACS) analysis using the BD Biosciences flow cytometer.

Measurement of mitochondrial membrane potential

Five thousand JB6 Cl-41 cells were seeded in 96-well plates. After 24 h of incubation, cells were treated with DMSO or TPA (5 nM) as indicated above. Twenty-four hours after the treatment, cells were washed with PBS and incubated in a fresh medium containing 2 µg/ml of 5,5′,6,6′-tetrachloro-1,1′,3,3′-tetraethylbenzimidazol-carbocyanine iodide (JC-1) for 30 min. The dye was then removed. Fluorescence intensity was measured immediately via fluorescence spectrometry (Synergy HT, BioTek, Winooski, VT). JC-1 dye exhibits potential-dependent accumulation in mitochondria, it changes color from red to green as the membrane potential decreases. Therefore, mitochondrial membrane potential correlates with the red/green fluorescence intensity ratio. For JC-1 green, Ex = 485 nm, Em = 528 nm; for JC-1 red, Ex = 530 nm, Em = 590 nm.

Assessment of Apoptosis via Annexin V staining

The percentage of apoptotic cells was determined by monitoring the translocation of phosphatidylserine to the cell surface using an Annexin V-FITC apoptosis detection kit (Sigma) according to the manufacturer's instructions. Cells were evaluated for apoptosis using a FACSCalibur flow cytometer (BD Biosciences) with Annexin V–FITC and PI double staining.

Real-time evaluation of apoptotic cell death

For activated caspase 3/7 apoptosis assays, JB6 Cl-41 cells were plated at 5,000 cells/well in 96-well plates for 24hours before treating with DMSO or TPA (5 nM). The caspase 3/7 reagent was added at a 1:1000 dilution (Essen Bioscience, Cat No. 4440, Ann Arbor, MI, USA). Cells were imaged at 10× magnification in an IncuCyte Zoom Live-content imaging system (Essen Bioscience) at 37°C, 5% CO_2. Images were acquired every 4hours over 3 days. Data were analyzed using IncuCyte analysis software to detect and quantify fluorescent (apoptotic) cells in each image. Each experiment was performed in triplicate.

Glucose uptake measurement

Cell culture supernatant (0.5 ml) was obtained before and after 24 h treatment with DMSO or TPA (5 nM) without disturbing the cells. ACCU-CHEK Active glucose test strips (Roche Diagnostics, Indianapolis, IN) were mounted onto the ACCU-CHEK Active glucose meter (Roche Diagnostics) and 20 µl of the supernatant sample was added to the sample loading area on the test strip. Glucose concentrations were calculated and reported as percentages.

Glucose PCR array

RNA was harvested from cells using Qiagen's RNeasy Micro Kit flowing the manufacturer's procedures. Synthesis of cDNA was conducted using Qiagen's RT2 First Strand Kit. An RT² Profiler Mouse Glucose PCR Array (Qiagen) was used to quantify the gene expression of the samples. Prepared cDNA from the reverse transcription was used in the array in combination with RT² SYBR® Green qPCR Mastermix from Qiagen. The array was conducted using a Bio-Rad CFX384 Touch Real-Time PCR system. Two 384-well plates were used for two sets of samples, n=4 per sample.

Data analysis was performed using the QIAGEN web portal at GeneGlobe. In brief, delta CT was calculated from the gene of interest and the average of reference genes. The resulting value was calculated to calculate the delta-delta CT from the delta CT (UCP2 overexpression) to delta CT (control group). The fold change was calculated using the formula $2^{-\Delta\Delta CT}$. The CT cut-off was set to 35 with a two-fold regulation threshold.

Statistical analysis

All experiments were repeated at least three times and each experimental group included at least three samples. Data were presented as the mean ± standard deviation (SD). Statistical software SAS 9.4 (SAS Institute Inc., Gary, NC) was used for all data analysis. One-way ANOVA followed by the Tukey–Kramer adjustment was used to examine differences among multiple groups. A p-value < 0.05 was regarded as statistically significant.

Results

Characterization of UCP2 overexpressed JB6 Cl-41 cells

In our previous studies, UCP2 expression was found to be amplified in human skin tumor tissue samples,[8] and UCP2 knockout suppressed skin tumor formation.[20] To study the mechanisms of how UCP2 upregulation promotes the early stage of skin tumorigenesis, we transfected JB6 Cl-41 mouse epidermal cells with a human UCP2-containing vector or the empty vector (pCMV6). After G418 selection, two clones from each vector transfection were randomly isolated (clones D1 and D3 for control pCMV cells and clones A1 and B3 for UCP2 overexpressed cells) and used for the following studies. As shown in Figure 1A, the protein levels of UCP2 were increased by approximately two-fold in both UCP2 overexpressed cells, which is consistent with that in human skin tumor tissues [8]. Next, mitochondrial membrane potential was detected to confirm the uncoupling effect. UCP2 overexpressed cells displayed decreased mitochondrial membrane potential compared to control cells (Figure 1B).

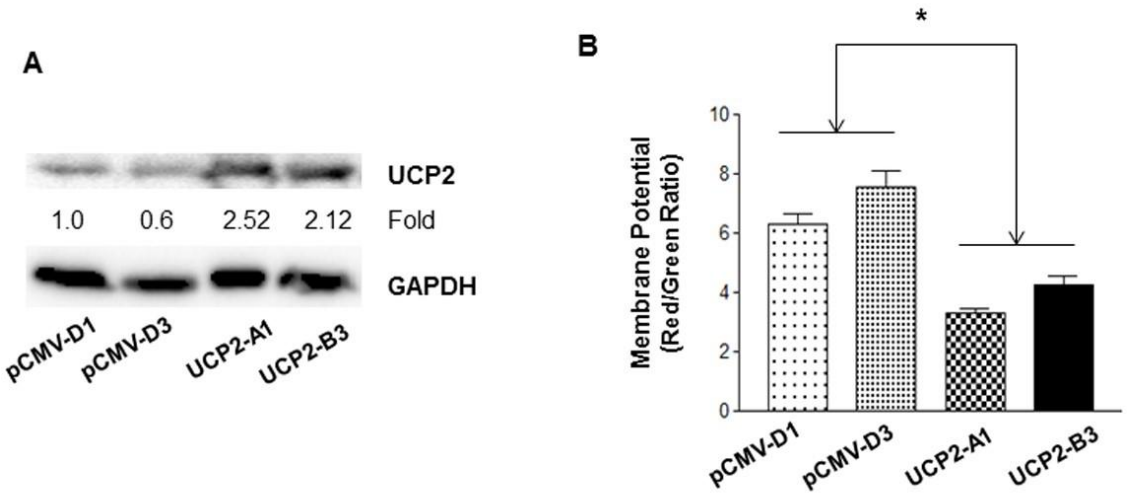

Figure 1. Characterization of UCP2 overexpressed JB6 Cl-41 cells

(A) The UCP2 expression levels were detected in two UCP2 overexpressed clones (UCP2-A1 and B3) and two empty-vector transfected clones (pCMV-D1 and D3). Whole cell lysates were used for the experiments and GAPDH served as the loading control.

(B) Mitochondrial membrane potential was measured by the JC-1 probe in pCMV and JB6 Cl-41 cells stably expressing UCP2. The results were presented as the mean ± SD of three independent experiments. One-way ANOVA with the Bonferroni post was used for statistical analysis. *, $p<0.05$ when any of the pCMV clones was compared with any of the UCP2 clones.

To evaluate whether UCP2 overexpression enhances cell transformation *in vitro*, anchorage-independent growth assays were performed. As shown in Figure 2A, the tumor promoter TPA induced colony formation in soft agar in both control pCMV cells and UCP2 overexpressed cells, and the number of colonies was significantly higher in UCP2 overexpressed cells compared to the control pCMV cells. Activator protein 1 (AP-1) activation is a driver for skin tumorigenesis.[23,24] The expression levels of Fra-1, a subunit of AP-1, were detected using Western blot analysis. As shown in Figure 2B, Fra-1 expression was induced by TPA treatment in control pCMV cells, which was further increased in UCP2 overexpressed cells. Taken together, this data indicates that we have successfully generated UCP2 stably overexpressed JB6 Cl-41 cells. The data generated from the pCMV-D3 and UCP2-A1 pairs were shown in the following studies, and data from the pCMV-D1 and UCP2-B3 pairs showed similar trends (data not shown).

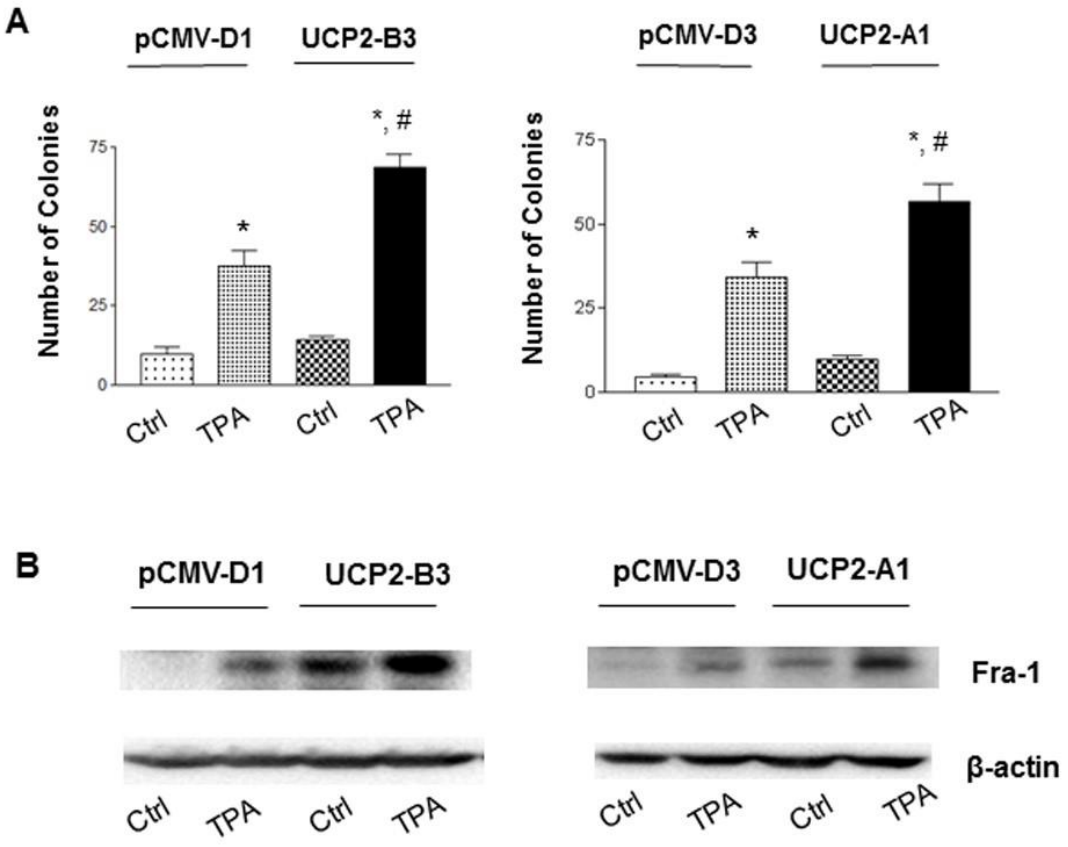

Figure 2. UCP2 overexpression promoted anchorage-independent growth and Fra-1 expression during skin cell transformation

(A) Soft agar assays were performed to detect anchorage-independent growth of the JB6 cells (n=3 in each group). Ctrl: vehicle (DMSO) treatment; TPA, 5 nM. *, $p<0.05$ when compared with its vehicle control group; #, $p<0.05$ when compared with the pCMV/TPA group.

(B) Western blot analysis to detect the expression levels of Fra-1 (a subunit of AP-1). β-actin was used as the loading control. Two UCP2 overexpressed colonies (UCP2-A1 and B3) and two empty-vector transfected colonies (pCMV-D1 and D3) were used in these studies.

UCP2 upregulation enhanced glucose uptake during skin cell transformation

Next, glucose uptake was measured to show whether UCP2 upregulation affects glucose metabolism. As shown in Figure 3, UCP2 overexpression significantly increased glucose consumption, and TPA treatment further enhanced this effect.

To determine which glucose metabolism-related genes are altered due to UCP2 overexpression, glucose PCR array analysis was performed, and the data showed that twenty genes were upregulated in UCP2 overexpressed cells compared to control cells, with glucose-6-phosphate dehydrogenase being the most upregulated gene (Table 1). Ten genes were downregulated by at least two folds in UCP2 overexpressed cells, but the changes were not statistically significant (data not shown).

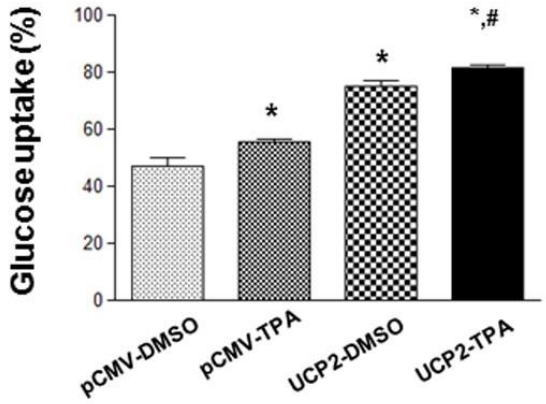

Figure 3. UCP2 overexpression enhanced glucose uptake during skin cell transformation
ACCU-CHEK active glucose meter was used to detect glucose uptake in control (pCMV-D3) and JB6 Cl-41 cells stably expressing UCP2 (UCP2-A1). Filtered Whole Cell Lysates were used in the experiments (n=3 per group). *, $p<0.05$ when compared with the pCMV/DMSO group; #, $p<0.05$ when compared with the pCMV/TPA group.

Table 1. Glucose metabolism-related genes that were upregulated in UCP2 overexpressed JB6 Cl-41 cells

Gene Name	Fold Change	p-Value
Aconitase 2	2.13	0.009572
Aldolase A	2.11	0.008003
2,3-bisphosphoglycerate mutase	2.20	0.004541
Dihydrolipoamide S-acetyltransferase	2.36	0.000344
Enolase 3	2.18	0.006160
Fumarate hydratase 1	2.06	0.014717
Glucose-6-phosphate dehydrogenase X-linked	12.65	0.005497
Glucan (1,4-alpha-), branching enzyme 1	2.04	0.001877
Glycogen synthase 1	2.33	0.001131
Hexokinase 2	2.86	0.010638
Isocitrate dehydrogenase 1	2.93	0.000147
Isocitrate dehydrogenase 3 alpha	2.35	0.000215
Phosphoenolpyruvate carboxykinase 2	3.29	0.000095
Phosphoglycerate kinase 1	2.07	0.000489
Phosphoglucomutase 1	2.16	0.000132
Phosphoglucomutase 2	2.44	0.000712
Phosphoglucomutase 3	2.15	0.003128
Phosphoribosyl pyrophosphate synthetase 1	3.48	0.000293
Succinate dehydrogenase complex, subunit B	2.05	0.020077
Triosephosphate isomerase 1	3.56	0.000122

Overexpression of UCP2 enhanced 3D cell growth

Since 3D spheroid formation is more representative of *in vivo* tumorigenesis than 2D culture, control pCMV and UCP2 overexpression JB6 Cl-41 cells were tested for their ability to form and grow as spheroids in 3D culture. As shown in Figure 4A and the quantification in Figure 4B, JB6 Cl-41 cells stably expressing UCP2 formed larger spheroids than control pCMV cells, TPA treatment also induced the formation of larger spheroids. Next, the UCP2 inhibitor genipin[25,26] was applied to JB6 Cl-41 cells stably expressing UCP2 in 3D spheroid culture. As shown in Figure 4C and the quantification in Figure 4D, genipin treatment reduced the sizes of spheroids formed by JB6 Cl-41 cells stably expressing UCP2 with or without TPA treatment, further supporting that UCP2 overexpression promotes skin cell transformation.

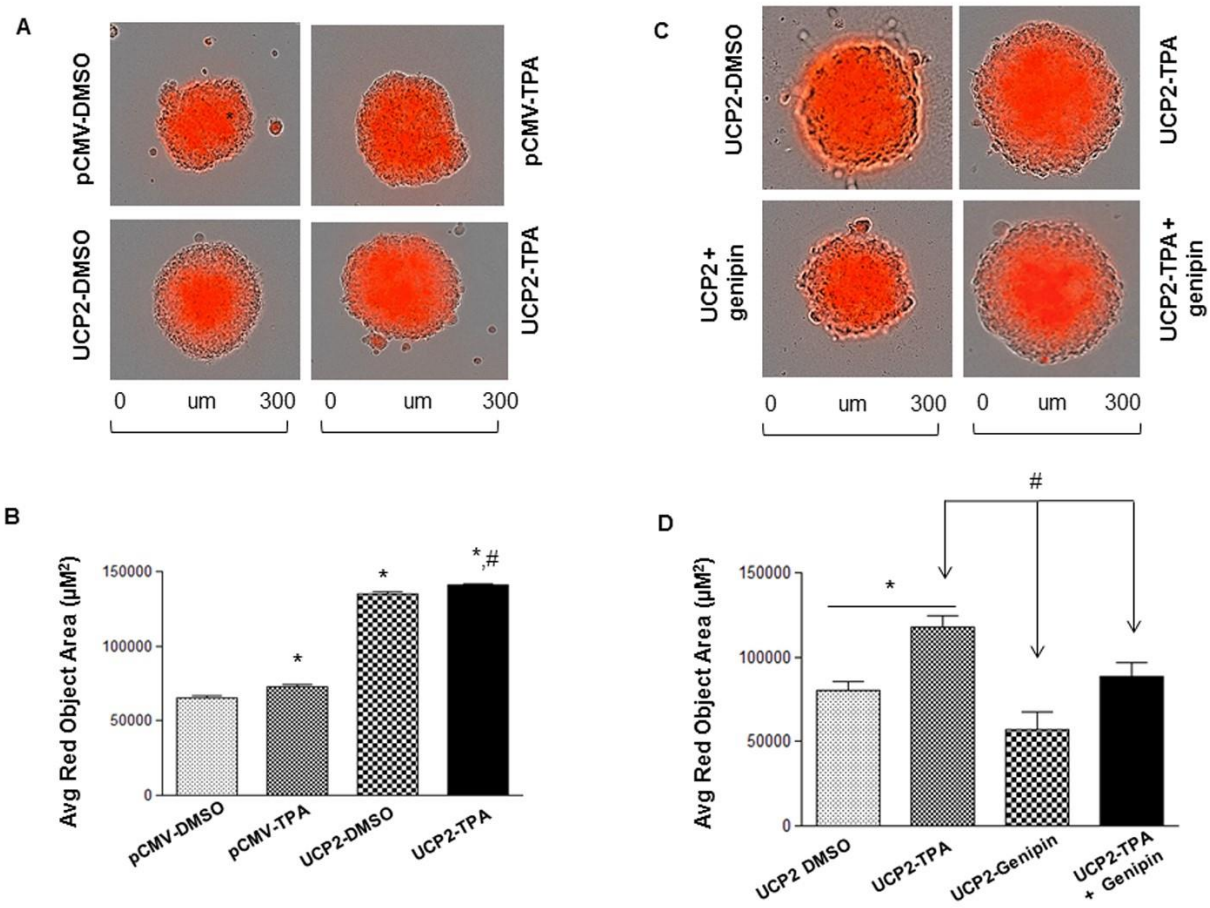

Figure 4. UCP2 overexpression promoted cell growth in 3D culture

(A) Representative fluorescent images of 3D spheroids and **(B)** image quantification of pCMV-D3 and UCP2-A1 cells after being treated with DMSO or TPA (5 nM) (n=6 in each group). *, $p<0.05$ when compared with the pCMV/DMSO group; #, $p<0.05$ when compared with the pCMV/TPA group.

(C & D) Similar experiments were performed in UCP2-A1 cells with or without the presence of genipin (10 μM) (n=6 in each group). Spheroid development in real time was monitored by taking images every 4 h in the IncuCyte ZOOM System. Quantification of spheroid was presented as average red object area expressed in μM^2. *, $p<0.05$ when compared with its control group; #, $p<0.05$ when compared with the UCP2/TPA group.

UCP2 overexpression increased the S-phase population during skin cell transformation

To study how UCP2 promotes cell growth, cell cycle analysis was performed using 3D spheroid cultures of control pCMV cells and JB6 Cl-41 cells stably expressing UCP2. The spheroids were dissociated into single cells after extraction and subjected to cell cycle analysis. Treatment with the tumor promoter TPA decreased the cell populations in the G1-phase in pCMV and JB6 Cl-41 cells stably expressing UCP2 (Figure 5A). Conversely, the same treatment increased the S-phase populations in pCMV and JB6 Cl-41 cells stably expressing UCP2 (Figure 5B). Furthermore,

cell numbers in the G2/M-phase were not significantly different between pCMV and JB6 Cl-41 cells stably expressing UCP2, and between the vehicle and TPA treatment (Figure 5C), although the percentage of cells in the G2/M phase appeared to be decreased in UCP2 overexpressed cells treated with TPA. Correspondently, the expression levels of Cyclin E, as well as that of Cdk2 (Cyclin E/Cdk2 complex drives cells into S-phase), were induced by TPA treatment in both pCMV and JB6 Cl-41 cells stably expressing UCP2 (Figure 5D). Interestingly, both TPA treatment and UCP2 overexpression also induced PTEN expression, which may partially counteract Cyclin E/Cdk2 activation, therefore cell cycle was not dramatically altered.

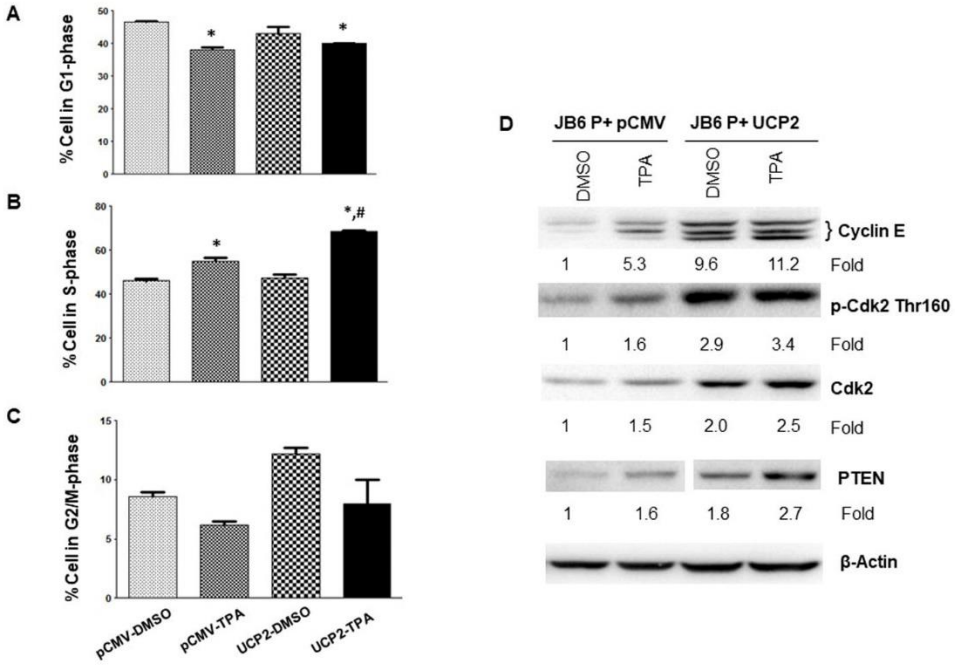

Figure 5. UCP2 overexpression increased the S-phase cell population

(A) Cell populations at G1-phase, **(B)** S-phase, and **(C)** G2/M-phase. Flow cytometry analysis was performed using dissociated 3D spheroid cultures of UCP2-A1 and pCMV-D3 cells. JB6 Cl-41 cells were allowed to form spheroids. The spheroids were treated with DMSO or TPA (5 nM) for 24 h, and the spheroids were harvested and dissociated into single cells. *, $p<0.05$ when compared with the pCMV-DMSO group; #, $p<0.05$ when compared with the pCMV-TPA group.

(D) Western blot analysis of Cyclin E, (p)Cdk2 and PTEN expression. The fold changes were included. β-actin was used as the loading control.

UCP2 overexpression did not suppress apoptosis during skin cell transformation

To study whether UCP2 overexpression suppresses apoptosis and therefore promotes cell transformation, JB6 Cl-41 cells stably expressing UCP2 and control pCMV cells were stained with Annexin V–FITC and Propidium Iodide, and the apoptotic cells were detected by flow cytometry. As shown in Figure 6A, the percentages of apoptotic cells were minimal, and there was no significant difference in the percentages of apoptotic cells between pCMV and JB6 Cl-41 cells stably expressing UCP2, with or without TPA treatment. Similarly, JB6 Cl-41 cells stably expressing UCP2 and control pCMV cells were treated with anti-caspase 3/7 antibodies and subjected to live-cell imaging. As shown in Figures 6B & 6C, UCP2 overexpression did not inhibit apoptosis. Therefore, these data suggest that inhibition of apoptosis may not be a mechanism for UCP2 to enhance cell transformation.

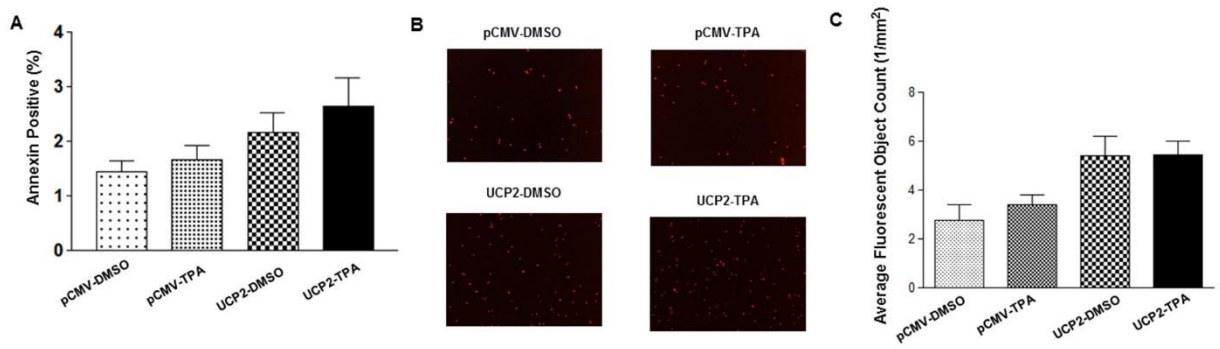

Figure 6. UCP2 overexpression did not inhibit apoptosis during skin cell promotion
The results of Annexin V staining **(A)** and active caspase 3/7 staining **(B & C)** were quantified and plotted. UCP2-A1 and pCMV-D3 cells were stained with Annexin V–FITC and PI (A) or active caspase 3/7 (B, quantified results shown in C). The percentages of apoptotic cells were detected by flow cytometry or the IncuCyte ZOOM system, respectively. The percentages of apoptotic cells were minimal, and no significant changes were detected.

Discussion

Cell proliferation, cell survival, and cell death constantly occur within an organism, and maintaining the balance between these events is imperative to homeostasis. Deregulation in either of these cellular processes can lead to the pathological conditions of cancer.[17,18,19] Cancer, a heterogeneous and extremely diverse disease, is characterized by uncontrolled growth, replicative immortality, genomic instability, enhanced cell proliferation, deregulated cellular bioenergetics, and resistance to apoptosis.[27] Deregulated cell proliferation and suppressed cell death provide a fundamental basis for tumor initiation and progression. Hence, it is critical to understand the molecular mechanism underlying such processes in tumorigenesis to develop novel therapeutic drugs.

Mitochondria and reactive oxygen species (ROS) are involved in regulating many critical cellular processes such as cell proliferation, cell survival, cell death, bioenergetics, and metabolism. Defective or dysfunctional mitochondria and/or altered ROS production contribute to tumor cell promotion, proliferation, and progression.[12,14,15] Recently, UCP2, a mitochondrial uncoupling protein, has gained more attention in the field of tumor biology due to its impact on mitochondria-dependent processes and redox regulation.[9] A growing body of evidence demonstrates that UCP2 is upregulated in some human cancers [8,28] and it has become a promising target for cancer therapy. It has been recognized that UCP2 can protect cancer cells against oxidative stress and drug-induced toxicity, change the metabolic behaviors of cancer cells, and modulate the anti-tumor immunity in the tumor microenvironment. Therefore, UCP2 may exhibit both pro- and anti-tumor activities in different types and stages of tumors.[28]

Using a chemically-induced skin carcinogenesis mouse model, our early studies have shown that loss of UCP2 expression suppresses skin tumor formation, which is the first to demonstrate that UCP2 knockout suppresses carcinogenesis *in vivo*.[20] Considering UCP2 is highly expressed in human skin cancer,[8] we have generated UCP2 overexpressed skin epidermal JB6 Cl-41 cells, to study how highly expressed UCP2 regulates skin tumor promotion, an early stage of skin tumorigenesis. The finding resulting from this study may help design a new strategy for cancer prevention.

We have published several findings using the UCP2 overexpressed JB6 cells, including: 1) UCP2 upregulation decreases superoxide but increases hydrogen peroxide production, which activates phospholipase C γ-1 (PLCγ-1), promoting skin cell transformation.[21] 2) UCP2 overexpression enhances glycolysis via Akt-dependent phosphor-fructokinase 2/fructose-2,6-bisphosphatase 2 (PFKFB2) activation.[22] However, how UCP2 upregulation affects the cell cycle to promote cell proliferation, whether UCP2 overexpression enhances glucose uptake, and whether UCP2 upregulation inhibits apoptosis during skin cell transformation have not been studied. The results from this study demonstrate that Fra-1/AP-1 activation, a critical oncogenic event during skin

carcinogenesis, is enhanced by UCP2 overexpression. Not surprisingly, UCP2 upregulation increases glucose uptake to fuel enhanced glycolysis. The S-phase cell population is increased, likely due to the increased expression of Cyclin E/Cdk2 in UCP2 overexpressed JB6 cells. UCP2 is shown to play an important role in the regulation of apoptosis through the alteration of redox balance.[29] In accordance with this hypothesis, Deng et al. showed that UCP2 reduced ROS-mediated apoptosis in A549 cells.[30] In this skin cell transformation model, UCP2 upregulation did not increase or decrease apoptosis, which is similar to what we have reported in the chemically-induced mouse skin carcinogenesis study, that UCP2 knockout does not increase or decrease apoptosis in mouse skin epidermal tissues.[20]

Conclusion

In this study, using a UCP2 overexpressed skin cell transformation model, our data indicate that UCP2 upregulation promotes cell proliferation at least partially mediated by enhancing the S-phase of the cell cycle, as well as by promoting glucose uptake and glycolysis. Our results also indicate that inhibition of apoptosis does not seem to be the mechanism for UCP2 to promote cell transformation.

Another important result is that genepin, a specific UCP2 inhibitor, could counteract the effects of UCP2 overexpression, which supports the effort of trying this inhibitor in treating UCP2 highly expressed cancers. In future studies, how highly expressed UCP2 regulates the expression of Cyclin E/Cdk2, and how UCP2 regulates glucose metabolism will be examined.

Conflicts of Interest

The authors declare no conflict of interest.

Acknowledgment

IncuCyte Zoom was provided by the Feist-Weiller Cancer Center'sInnovative North Louisiana Experimental Therapeutics program (INLET)directed by Dr. Glenn Mills at LSUHSC-S and supported by the LSU Health Shreveport Foundation. We thank Dr. Ana-Maria Dragoi,Associate Director of INLET, and Dr. Jennifer Carroll, Director of the*In Vivo, In Vitro*Efficacy Core for their assistance in IncuCyte studies.

Author Contributions

A.S., C.Z., and N.J: performed the experiments and analyzed the data. A.S. and Y.Z.: wrote the manuscript.

References

1) Rousset S, Alves-Guerra MC, Mozo J, et al. The biology of mitochondrial uncoupling proteins. *Diabetes*. 2004;53(suppl 1):S130-135.
2) Fleury C, Neverova M, Collins S, et al. Uncoupling protein-2: a novel gene linked to obesity and hyperinsulinemia. *Nat Genet*. 1997;15:269-272.
3) Brand MD, Esteves TC. Physiological functions of the mitochondrial uncoupling proteins UCP2 and UCP3. *Cell Metab*. 2005;2:85-93.
4) Sreedhar A, Zhao Y. Uncoupling protein 2 and metabolic diseases. *Mitochondrion*. 2017; 34:135-140.
5) Horimoto M, Resnick MB, Konkin TA, et al. Expression of uncoupling protein-2 in human colon cancer. *Clin Cancer Res*. 2004;10:6203-6207.
6) Derdak Z, Mark NM, Beldi G, et al. The mitochondrial uncoupling protein-2 promotes chemoresistance in cancer cells. *Cancer Res*. 2008;68:2813-2819.
7) Trachootham D, Alexandre J, Huang P. Targeting cancer cells by ROS-mediated mechanisms: a radical therapeutic approach? *Nat Rev Drug Discov*. 2009;8:579-591.
8) Li W, Nichols K, Nathan CA, et al. Mitochondrial uncoupling protein 2 is up-regulated in human head and neck, skin, pancreatic, and prostate tumors. *Cancer Biomark*. 2013;13:377-383.
9) Valle A, Oliver J, Roca P. Role of uncoupling proteins in cancer. *Cancers*. 2010;2:567-591.
10) Colburn NH, Bruegge WV, Bates JR, et al. Correlation of anchorage-independent growth with tumorigenicity of chemically transformed mouse epidermal cells. *Cancer Res*. 1978;38:624-634.
11) Sadikovic B, Al-Romaih K, Squire JA, et al. Cause and consequences of genetic and epigenetic alterations in human cancer. *Curr Genomics*. 2008;9:394-408.
12) Boland ML, Chourasia AH, Macleod KF. Mitochondrial dysfunction in cancer. *Front Oncol*. 2013;3:292.
13) Brookes PS, Yoon Y, Robotham JL, et al. Calcium, ATP, and ROS: a mitochondrial love-hate triangle. *Am J Physiol Cell Physiol*. 2004;287:C817-833.
14) Carew JS, Huang P. Mitochondrial defects in cancer. *Mol Cancer*. 2002;1:9.
15) Modica-Napolitano JS, Singh KK. Mitochondrial dysfunction in cancer. *Mitochondrion*. 2004;4:755-762.
16) Wallace DC. A mitochondrial paradigm of metabolic and degenerative diseases, aging, and cancer: a dawn for evolutionary medicine. *Annu Rev Genet*. 2005;39:359-407.
17) King KL, Cidlowski JA. Cell cycle and apoptosis: common pathways to life and death. *J Cell Biochem*. 1995;58:175-180.
18) Evan GI, Vousden KH. Proliferation, cell cycle and apoptosis in cancer. *Nature*. 2001;411:342-348.
19) Maddika S, Ande SR, Panigrahi S, et al. Cell survival, cell death and cell cycle pathways are interconnected: implications for cancer therapy. *Drug Resist Updat*. 2007;10:13-29.
20) Li W, Zhang C, Jackson K, et al. UCP2 knockout suppresses mouse skin carcinogenesis. *Cancer Prev Res*. 2015;8:487-491.
21) Sreedhar A, Lefort J, Petruska P, et al. UCP2 upregulation promotes PLCγ-1 signaling during skin cell transformation. *Mol Carcinog*. 2017;56:2290-2300.
22) Sreedhar A, Petruska P, Miriyala S, et al. UCP2 overexpression enhanced glycolysis via activation of PFKFB2 during skin cell transformation. *Oncotarget*. 2017;8:95504-95515.
23) Bernstein LR, Colbrun NH. AP1-jun function is differently induced in promotion-sensitive and resistant JB6 cells. *Science*. 1989;244:566-570.
24) Dong Z, Birrer MJ, Watts RG, et al. Blocking of tumor promoter-induced AP-1 activity inhibits induced transformation in JB6 mouse epidermal cells. *Proc Natl Acad Sci USA*. 1994;91:609-613.
25) Fujikawa S, Nakamura S, Koga K. Genipin, a new type of protein crosslinking reagent from gardenia fruits. *Agricultural and biological chemistry*. 1988;52:869-870.
26) Qiu W, Zhou Y, Jiang L, et al. Genipin inhibits mitochondrial uncoupling protein 2 expression and ameliorates podocyte injury in diabetic mice. *PLoS One*. 2012;7:e41391.
27) Hanahan D, Weinberg RA. Hallmarks of cancer: the next generation. *Cell*. 2011;144:646-674.
28) Luby A, Alves-Guerra MC. UCP2 as a Cancer Target through Energy Metabolism and Oxidative Stress Control. Int J Mol Sci. 2022 Dec 1;23(23):15077.
29) Ge H, Zhang F, Shan D, et al. Effects of mitochondrial uncoupling protein 2 inhibition by genipin in human cumulus cells. *Biomed Res Int*. 2015;2015:323246.

30) Deng S, Yang Y, Han Y, et al. UCP2 inhibits ROS-mediated apoptosis in A549 under hypoxic conditions. *PLoS One.* 2012;7:e30714.